REPORT NO. 3

NASA RESEARCH GRANT

NGL 22-011-024

REPORT NO. 3

NASA RESEARCH GRANT NGL 22-011-024

A STUDY OF MICROMINIATURIZED DEVICES FOR BIOASTRONAUTICAL MONITORING OR ANALYSIS

by

B. L. Cochrun

J. S. Rochefort

Electronics Research Laboratory

Northeastern University

Boston, Massachusetts

1 March 1969

The research reported here was sponsored by the National Aeronautics and Space Administration under Research Grant NGL 22-011-024 for the period from 1 September 1968 through 28 February 1969. This report is published for information purposes only and does not represent recommendations or conclusions of the sponsoring agency. Reproduction in whole or part is permitted for any purpose of the United States Government.

RESEARCH STAFF

Basil. L. Cochrun, Co-principal Investigator
Associate Professor of Electrical Engineering

J. Spencer Rochefort, Co-principal Investigator
Professor of Electrical Engineering

K. Hergenrother
Research Associate

H. Mahdi
Phd. Candidate

I. Introduction

Since the last report, Report No. 2, progress has been made in the areas of active circuit synthesis using RC distributed networks, d-c to d-c converters, digital filters and a preliminary oximeter using electro-luminescent solid state diodes in a pulsed mode of operation.

The problem of miniaturization using hybrid techniques has been under investigation. This has involved the search for suitable substrates and chip components such as transistors, resistances and capacitors. The latter two items are in hand. The principal component problem is the availability of the necessary FET's in chip form at a reasonable cost. The required units are available only in large quantities and at a prohibitive cost. The difficulty may be ameliorated by the progress achieved in the d-c to d-c converters which will make less necessary the tight restrictions on the FET's now being used in the modular buffer amplifier.

II. Active Circuit Synthesis

Mr. H. Mahdi's doctoral thesis proposal was accepted by the Electrical Engineering Faculty of Northeastern University and he has continued his work involved with the synthesis of active circuits using distributed RC networks.

During this period, synthesis of RC distributed active circuits using exponentially tapered RC distributed networks, $\overline{ERC}$, were investigated. Since $\overline{ERC}$ distributed networks offer far better roll off than uniform RC distributed network, $\overline{URC}$, the original intension was to achieve third order Butterworth magnitude response by replacing the $\overline{URC}$ in Figure 1 with an $\overline{ERC}$. The system voltage transfer function of the circuit in Figure 1 using $\overline{ERC}$ can be expressed as

$$T_{(s)} = \frac{V_3}{V_1} = \frac{\frac{K}{1-K}}{(\cosh\theta + \frac{\alpha d}{2\theta}\sinh\theta)\, e^{\frac{-\alpha d}{2}} + \frac{K}{1-K}} \qquad (1)$$

where $\theta = \sqrt{(\frac{\alpha d}{2})^2 + ST_o}$

αd = tapering factor

and T_o = per unit length time constant.

A plot of the magnitude response of the system transfer function given in equation (1) under maximally flat magnitude conditions showed a roll off of 13dB per octave rather than 18dB which is the required cut off rate for the third order Butterworth magnitude response. Although the magnitude response is not effected as the tapering factor, αd, is increased, the phase response is substantially linearized. Furthermore, since the magnitude response is not effected substantially by the tapering factor, it is possible to synthesize the magnitude response of a pair of complex conjugate poles at any pole angle using $\overline{ERC}$ networks.

It is felt that these circuits could be used for the synthesis of low-pass filters having the magnitude response of Butterworth functions and the phase linearity associated with the transitional Butterworth-Thomson functions. They could be used for the simultaneous realization of magnitude response of

low-pass Thomson filters having the phase linearity associated with higher order Thomson functions. These characteristics are not obtainable from lumped RC active synthesis.

Another advantage achieved by using $\overline{ERC}$ networks is the reduction of the gain required for the realization of a pair of complex conjugate poles at any pole angle. Since the sensitivity of Q (pole quality) to changes in gain is defined as

$$S_K^Q = \frac{\Delta Q/Q}{\Delta K/K} = \frac{K}{Q} \frac{\Delta Q}{\Delta K} \tag{2}$$

this could mean that lower Q sensitivity to changes in gain can be achieved by using $\overline{ERC}$ networks. Reduction in gain and improvement in Q sensitivity to changes in gain makes these circuits attractive for high-frequency applications.

At this time the details of the progress in this area are being prepared for submission to the IEEE Transactions on Circuit Theory for publication as two papers. The first paper would be concerned with the work on active synthesis using $\overline{URC}$ networks. It would include design tables based on dominant poles of the transfer function rather than those obtained by matching the magnitude response of the system transfer function of Figure 1 with a pair of complex conjugate poles (see Table 1), the effect of the non-dominant poles on phase and transient response and Q sensitivity to variations in gain at all pole angles.

The second paper will cover the synthesis of linear phase low-pass transfer functions using exponentially RC distributed networks. The subject matter will include (1) design tables based on magnitude response matching techniques; (2) calculation of phase linearity as a function of tapering factor αd and study of Q sensitivity to variation in gain K and tapering factor αd; (3) realization of low-pass filters having maximally flat magnitude response and possibly maximally flat group delay.

III. D-c to D-c Converters

It was noted in the last semi-annual report that significant improvement in the characteristics of the modular buffer amplifier was possible by operating at voltages greater than that of the mercury cell (i.e. 1.3 volts). In view of this fact effort was intensified to obtain larger voltages while still using single mercury cells as the primary source of power.

Any approach requiring transformers did not appear feasible on the basis of size and weight limitations. The conventional approach using diodes in typical doubler circuits, such as is illustrated in Figure 3, could not be employed because of the prohibitively large junction voltages associated with the diodes, (0.3 to 0.6 volts for germanium and silicon respectively), which are comparable to the potential of the mercury cell. Bipolar transistors, on the other hand, appeared quite attractive for this application since they have saturation characteristics which make them useful as near ideal switches. For example there are some transistors available which have collector-to-emitter saturation voltages less than 50 millivolts.

These considerations led to the basic circuit of Figure 4 which uses bipolar transistors as switches operating in the saturation mode. The switching voltages E_s and $\overline{E}_s$ are 180^o out of phase with a maximum voltage equal to the d-c supply voltage V_s. With E_s=0 volts, C_1 charges to $V_s - V_{CE1}(sat)$. With $E_s = V_s$ and $\overline{E}_s$=0 volts the voltage at point A reaches $2V_s - V_{CE1}(sat)$ and C_2 charges to $2V_s - 2V_{CE}(sat)$, assuming equal saturation voltage for the two transistors. Using transistors with saturation voltages of 10 millivolts, circuits have been constructed which give output voltages of 2.68 volts when a supply voltage of 1.35 volts is used.

The original switching voltage was obtained from a commercial laboratory pulser. Having proven the feasibility of this approach to voltage doubling, attention was given to incorporating the clock switching circuit as an integral part of the complete converter. Based upon the experience gained from the design of the buffer amplifier, it was decided to develop a free running multivibrator which would operate from the common supply voltage of 1.3 volts. The clock circuit designed for this purpose is shown in Figure 5. For the circuit values shown, a square wave output voltage was obtained having rise and fall times of 30 and 20 nanoseconds respectively with an input current of 1ma.

A complete prototype doubler circuit is shown in Figure 6. The circuit characteristics are shown in Table II. With V_S=1.35 volts, an output voltage of 2.52 volts was obtained for a load current of 1.25ma. The efficiency for these conditions is 55.7%.

Extension of this basic concept is possible to obtain even higher voltages. An experimental quadrupler circuit was built which gave close to four times the input voltage. This was achieved by merely cascading two additional switching circuits with the original two of the doubler circuit.

IV. Digital Filters

The first stage of the digital filter investigation was completed during the previous report period. Parameter variation had been studied and the conclusion had been reached that appropriate filters were feasible. The second stage of the study was proposed for this report period and was to encompass the effect of component size and availability upon design.

First degree Butterworth filters have been constructed utilizing resistors, operational amplifiers and capacitors. One filter was constructed utilizing 5% off-the-shelf carbon resistors while a second utilized hand-selected values. Although Butterworth responses were realized in both instances, the cut-off frequency was 15% removed from the desired value when 5% resistors were used, but was within 1.5% when selected resistors were employed.

As indicated in the previous report, the Z-transform of a first degree Butterworth filter can be expressed as

$$\frac{Y(Z)}{X(Z)} = \frac{a\,Z^{-1}}{1-b\,Z^{-1}} \tag{3}$$

where Y(Z) and X(Z) are the respective Z-transforms of output and input, a and b are weighted coefficients, and Z represents e^{sT} with the T the period of the sampling waveform. This equation may be rewritten as

$$Y(Z) = a\,W(Z)\,Z^{-1} \tag{4}$$

where

$$W(Z) = X(Z) + b[W(Z)\,Z^{-1}]\,. \tag{5}$$

The inverse transform of (5) for the n^{th} data sample becomes

$$w_n = x_n + b\,w_{n-1} \tag{6}$$

and can be realized as indicated in Figure 7a with an adding circuit, an amplifier of gain b, and a delay T. With equation (6) thus realized the time response

indicated by (4) can be obtained by merely following the output from the system shown in Figure 7a with an amplifier of gain a. Since a linear circuit is involved, however, the same result is obtained if the amplifier is inserted before the adder as indicated in Figure 7b. This latter configuration can be readily handled in the adder synthesis.

The actual prototype filter was constructed with Analog Devices 141A operational amplifiers and M100 field effect transistors and is shown in Figure 7c. The adding circuit is comprised of resistors R_1 and R_2 working into the extremely high input impedance of the first 141A amplifier. The sizes indicated allow values of a=1-b and b=.544 to be realized. These values set the cut-off frequency at one tenth the input data rate. A General Radio Type 1210B RC Oscillator was used to generate a 10kHz square wave, φ, and its compliment, $\bar{\varphi}$. These waveforms served to sample the input data, store the current sum of $ax_n + by_{n-1}$ on C_1, and then shift this sum to C_2 a half period later to generate the new y_n. The output shown should be followed by a crude low-pass filter to eliminate the pass-bands which are centered about the harmonics of the sampling frequency. This filter was omitted from this model but will be employed with most higher order types.

It should be noted that the operational amplifiers are used as unity gain, non-inverting isolators and thus in any final design can be replaced by simple isolation circuits. The capacitance sizes are not critical provided that the associated time constants are small enough to allow quick charging during one half-period and then become large enough to retain the resulting voltage for the next half-period of the sampling frequency. The General Radio sampling source can be readily replaced with a compact astable multivibrator in any final package. Consequently, the resistors R_1 and R_2 remain as the only critical elements. When the design values of these components were synthesized with off-the-shelf 5% carbon resistors, a cut-off frequency of 850Hz was obtained. When an ohmmeter was used to select component sizes to provide 11.9K and 10.0K resistances, a cut-off frequency of 985Hz was realized. In a final system hybrid circuitry would probably be used and the required tolerances for resistance values are within the state of the art.

V. Prototype Oximeter

The preliminary oximeter circuit consists of a dual pulser, two light diodes and a photo-diode-operational-amplifier detector.

The dual pulser, which was designed and constructed here at Northeastern, is capable of driving the light diodes independently with the outputs out of phase. The individual outputs are current sources with the output current continuously variable from 0-150ma. The circuit is shown in Figure 8.

The light diodes were fabricated here at Northeastern by Mr. Hergenrother. One diode emits light at 8200 Å and the other 6700 Å. They are mounted in a TO-5 header in close approximity to each other and sealed over with clear epoxy.

The detector is a commercial EGG combination photodiode and operational amplifier model HAD-130.

The initial tests of this system centered on attempting to evaluate the necessary pulse amplitude to achieve satisfactory operation in terms of signal-to-noise ratio. The primary source of noise appears to be that due to the photo diode. Noise was also encountered with the operational amplifier because of its large feedback resistance, however, this was of minor importance compared to the unacceptable level of d-c offset voltage. The latter seriously affected the dynamic range of operation of the amplifier. Additionally, the photodiode appeared unduly sensitive to temperature variation.

Consideration was given to designing an amplifier to follow the photodiode, however, it was felt that from the viewpoint of time it would be more expedient to temperature stabilize the existing commercial detector.

Despite the problems encountered to this point the preliminary tests are encouraging. Rather crude transmission tests using human skin do show a variation in the amplitude of the transmitted light pulses at the two different wavelengths. More definitive results will be possible once the detector difficulties are surmounted.

VI. Projections

Work on the d-c to d-c converters will be extended in an attempt to obtain operation at lower input voltages than that of the mercury cell. This will be necessary when nuclear cells with 0.4 volts potential become available in the future. Extension of the present effort will also be made to obtain dual polarity output voltages with single cells as the primary input power.

The design approach, circuit configurations and experimental techniques which were developed along with the prototype simple analog filter will enable quicker progress to be made in obtaining higher order filters. Development of prototype second and third order Butterworth filters, which is in progress, will be continued. Consideration will also be given to binary coded digital filters.

Work on the prototype oximeter will be intensified. There is a good possibility that a graduate student can be assigned to this project to do a thesis on a full time basis. Arrangements are being made to obtain tissue and blood samples for transmission and reflection tests once the stability problems have been solved.

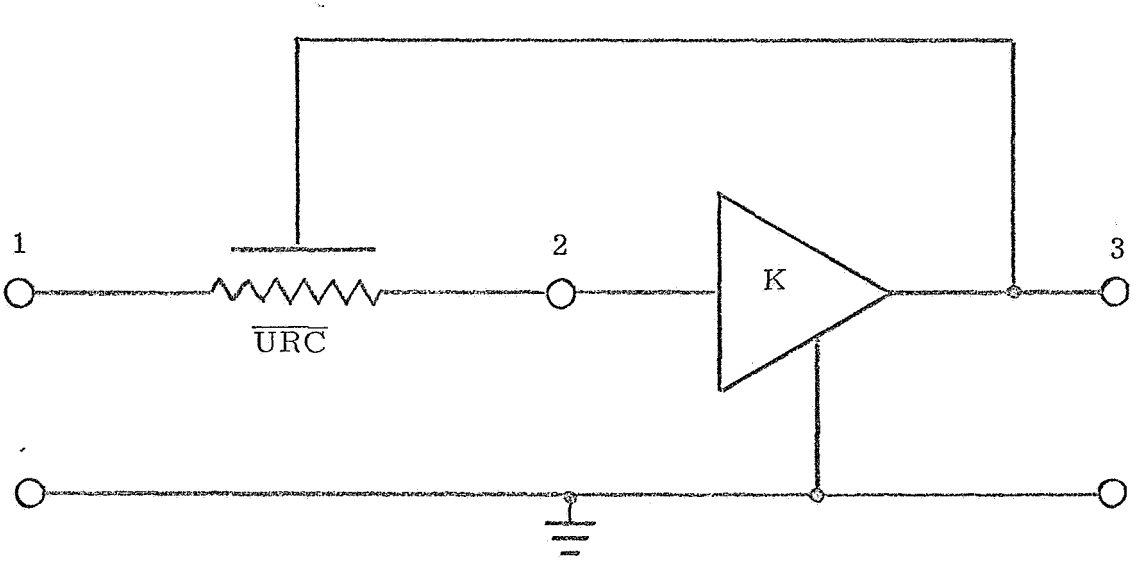

Figure 1. Active distributed RC circuit using $\overline{\text{URC}}$ network of total time constant T_o.

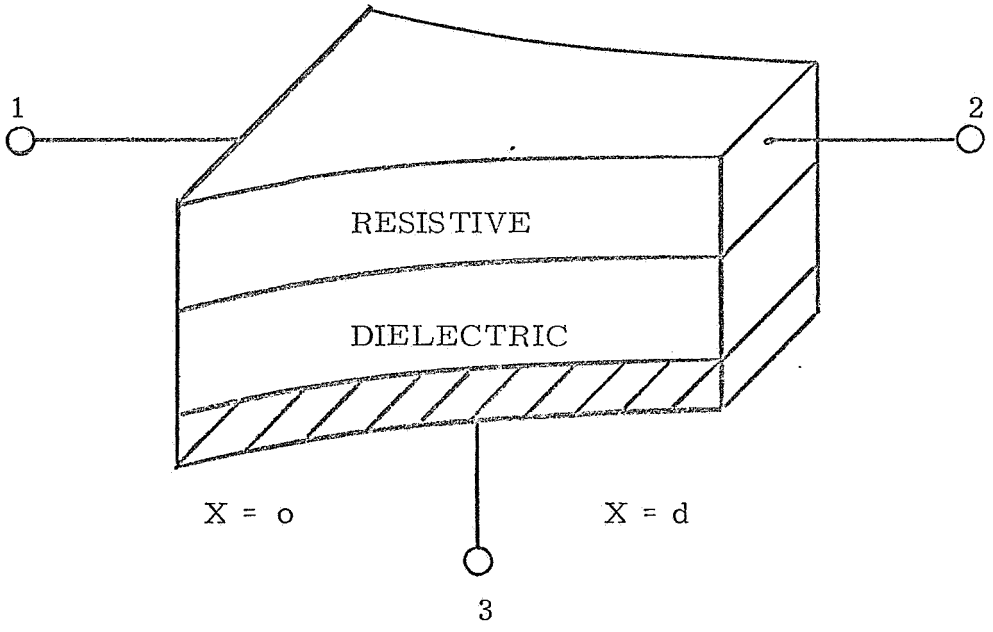

Figure 2. An exponentially tapered thin-film network having per unit length resistance and capacitance of $r(x) = r_0 e^{\alpha x}$ and $c(x) = c_0 e^{-\alpha x}$ respectively.

Table 1. Required K and T_{on} for synthesis of a pair of complex conjugate poles at pole angle γ.

Pole Angle γ	K	T_{on}	Pole Angle γ	K	T_{on}
1	.500	9.870	46	.670	11.648
2	.500	9.873	47	.676	11.736
3	.501	9.876	48	.682	11.826
4	.502	9.882	49	.689	11.919
5	.502	9.888	50	.695	12.016
6	.503	9.897	51	.701	12.115
7	.505	9.907	52	.708	12.217
8	.506	9.918	53	.714	12.323
9	.508	9.931	54	.721	12.432
10	.509	9.945	55	.727	12.544
11	.511	9.961	56	.733	12.660
12	.513	9.979	57	.740	12.779
13	.516	9.998	58	.746	12.902
14	.518	10.018	59	.753	13.029
15	.521	10.041	60	.759	13.159
16	.524	10.065	61	.765	13.294
17	.527	10.090	62	.772	13.433
18	.530	10.117	63	.778	13.576
19	.533	10.146	64	.784	13.723
20	.536	10.176	65	.790	13.875
21	.540	10.209	66	.796	14.032
22	.544	10.242	67	.802	14.193
23	.548	10.278	68	.808	14.360
24	.552	10.315	69	.814	14.532
25	.556	10.355	70	.820	14.709
26	.560	10.396	71	.826	14.891
27	.565	10.438	72	.832	15.079
28	.569	10.483	73	.838	15.274
29	.574	10.530	74	.843	15.474
30	.579	10.578	75	.849	15.681
31	.584	10.629	76	.854	15.894
32	.589	10.681	77	.860	16.114
33	.594	10.736	78	.865	16.342
34	.600	10.792	79	.870	16.576
35	.605	10.851	80	.875	16.819
36	.611	10.912	81	.880	17.069
37	.616	10.975	82	.885	17.328
38	.622	11.040	83	.890	17.595
39	.628	11.107	84	.895	17.871
40	.633	11.177	85	.899	18.157
41	.639	11.249	86	.904	18.452
42	.645	11.324	87	.908	18.757
43	.651	11.401	88	.912	19.074
44	.657	11.481	89	.917	19.401
45	.664	11.563	90	.921	19.739

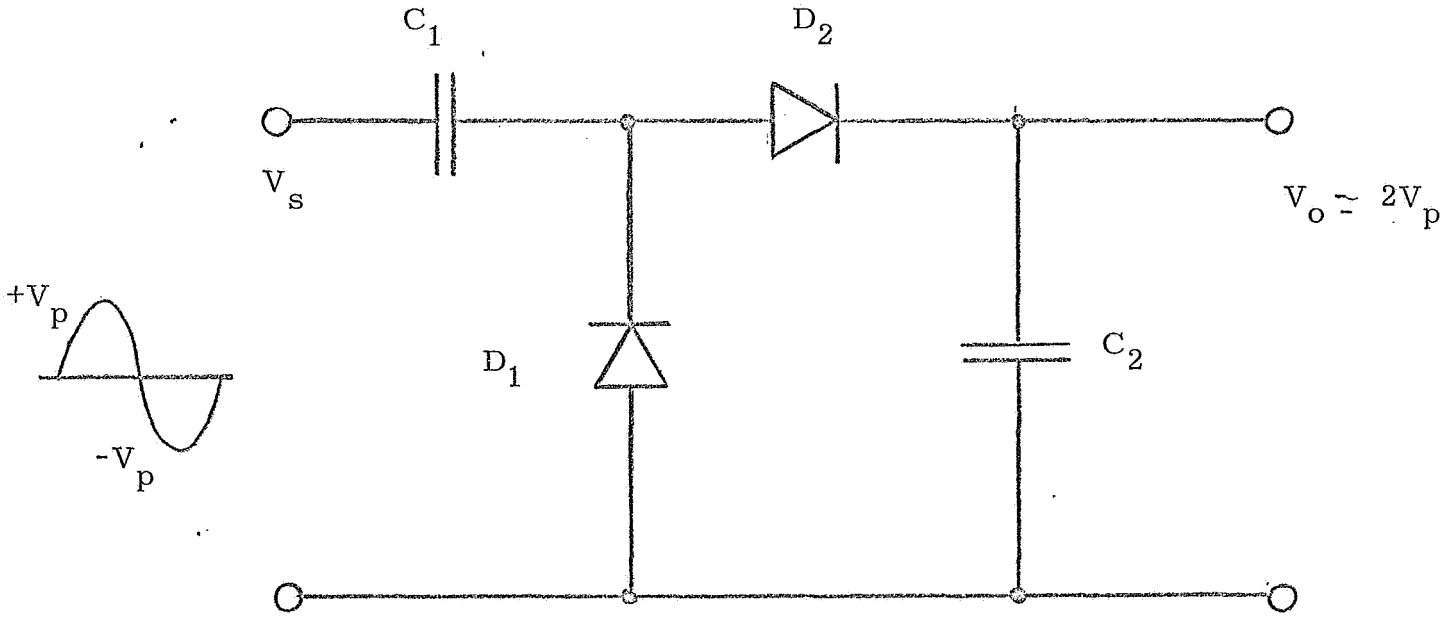

Figure 3. Typical voltage doubler circuit.

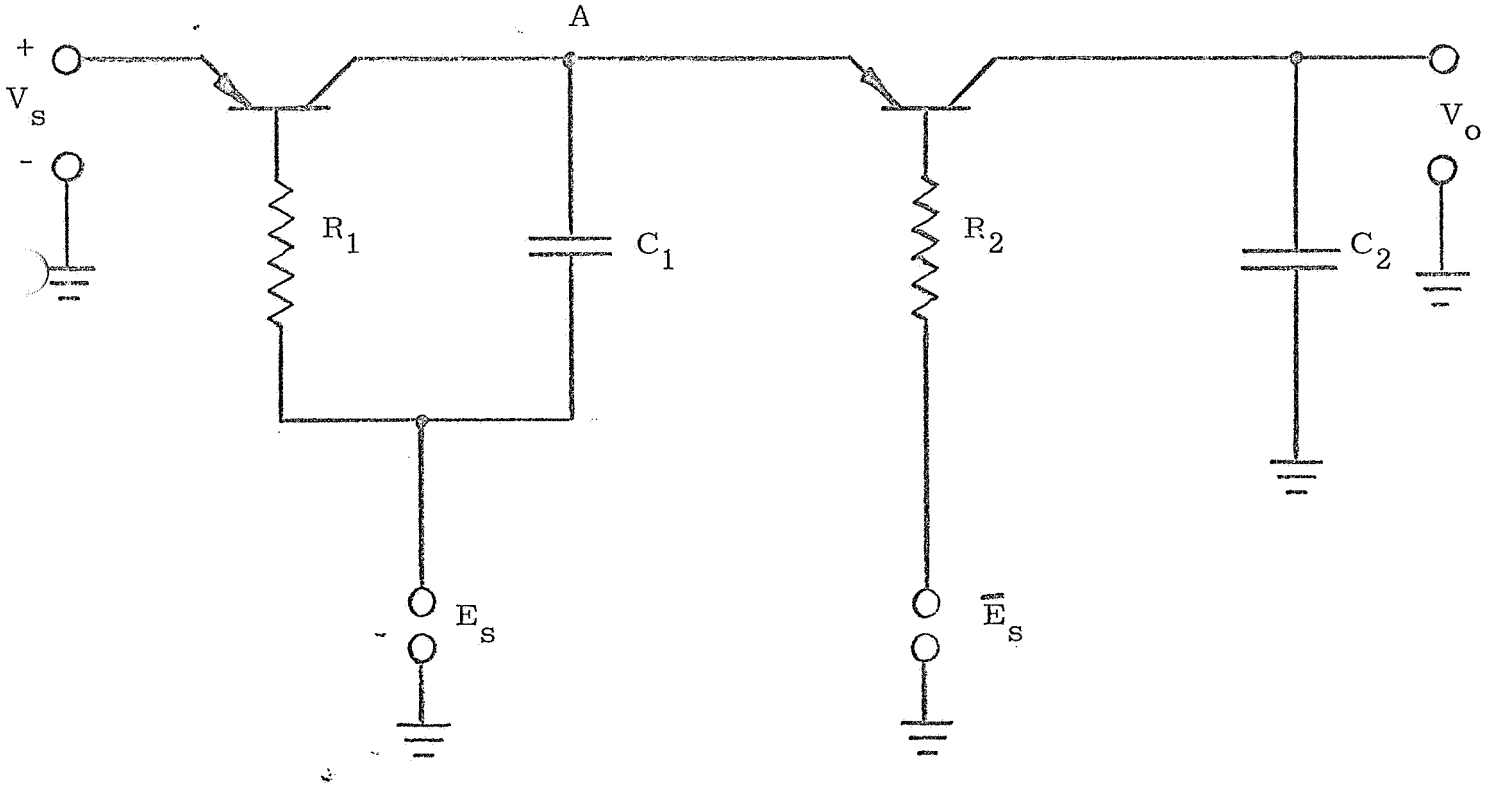

Figure 4. Voltage doubler using bipolar switches in saturation mode.

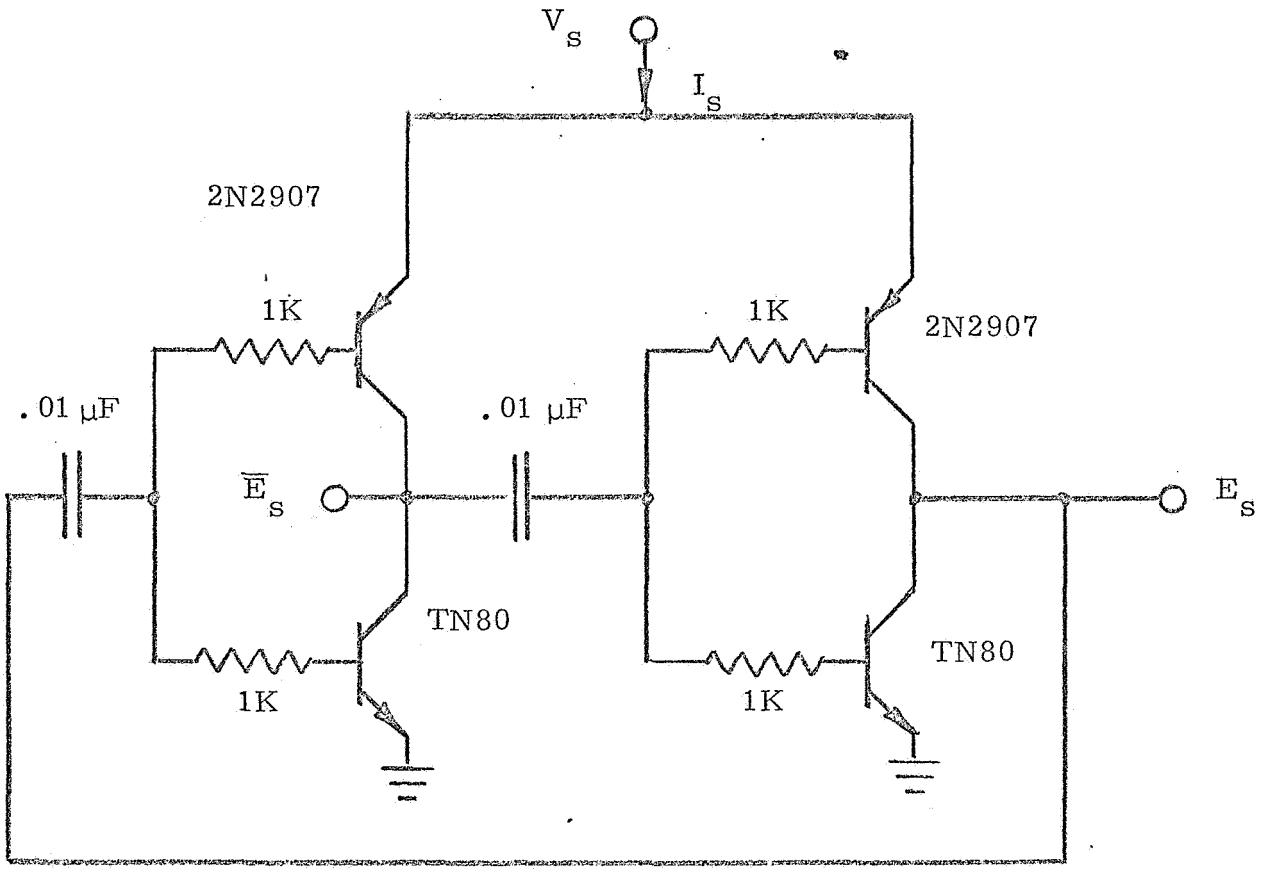

Figure 5(a). Voltage doubler clock circuit.

V_s (volts)	I_s (ma)	t_r (ns)	t_f (ns)
1.25	0.5	50	20
1.35	1.0	30	20
1.45	1.7	30	20

Figure 5(b). Circuit characteristics of Figure 5(a).

Figure 5. Voltage doubler clock circuit and its characteristics, (a) circuit - (b) characteristics.

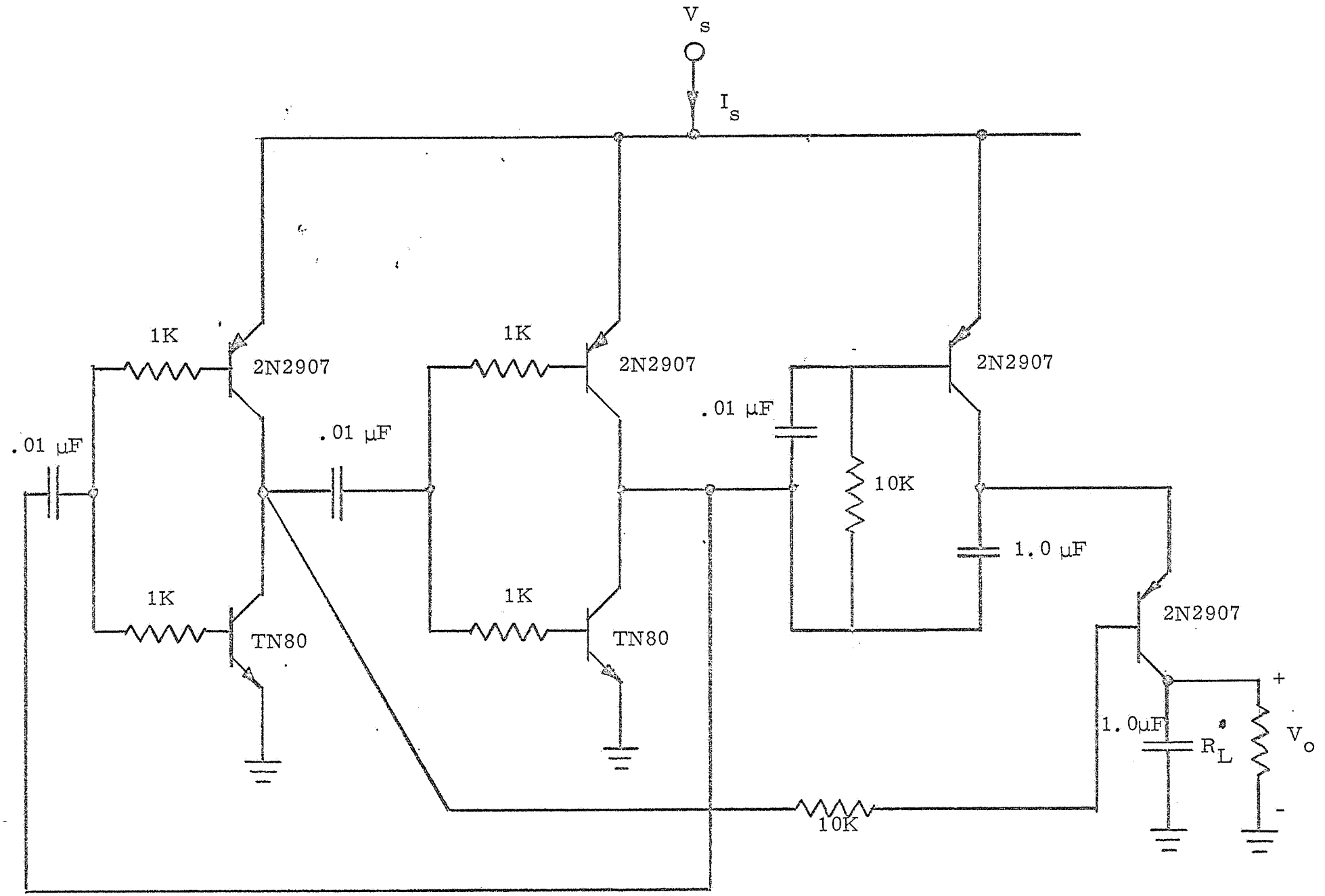

Figure 6. Complete voltage doubler circuit.

TABLE II

Load (ohms)	I_s (ma)	V_o (volts)	Efficiency (%)
∞	2	2.623	0.0
20K	2.2	2.609	11.5
10K	2.4	2.598	20.8
5K	2.8	2.577	35.2
3K	3.5	2.548	45.8
2K	4.2	2.516	55.7

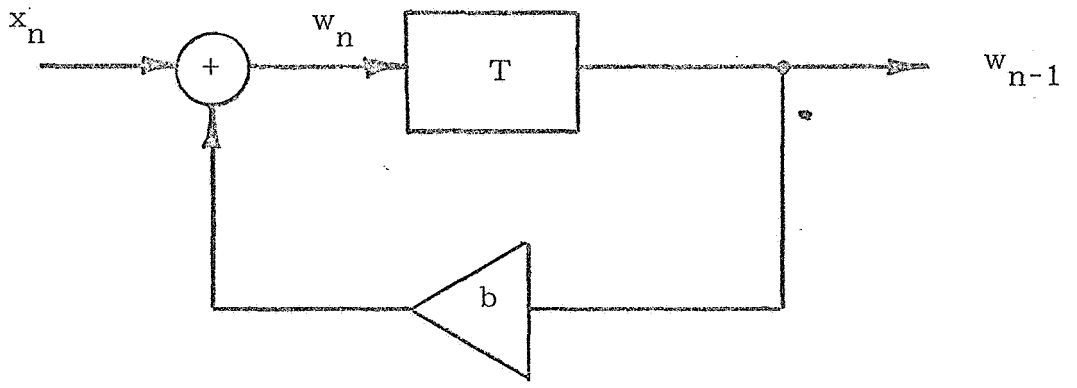

Figure 7a. Analog Version of Equation (6)

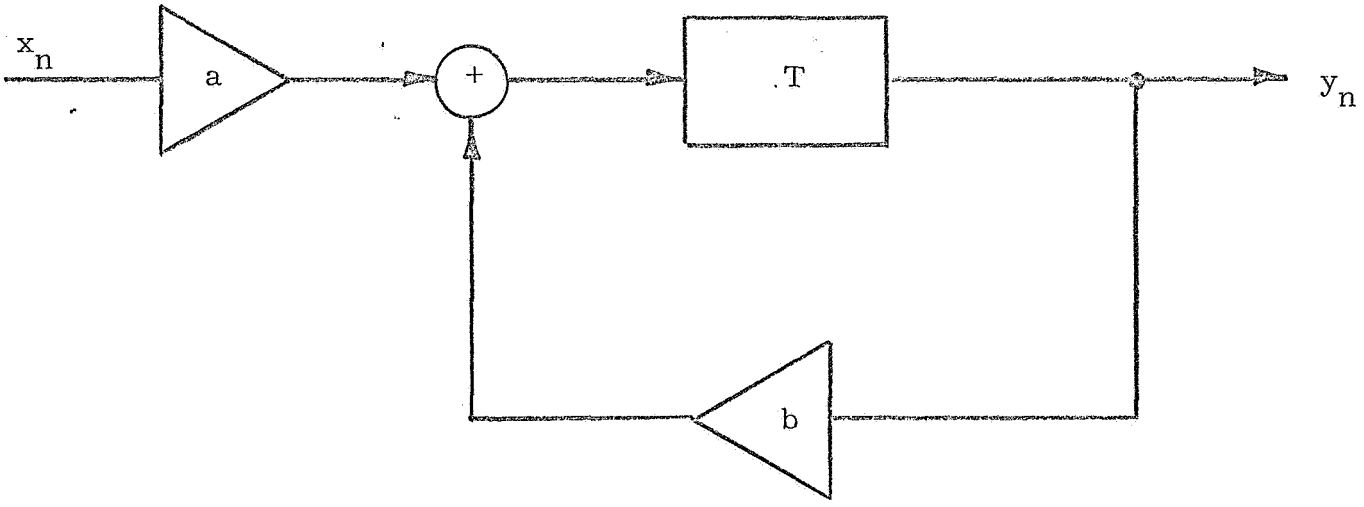

Figure 7b. Block Diagram of First Degree Filter

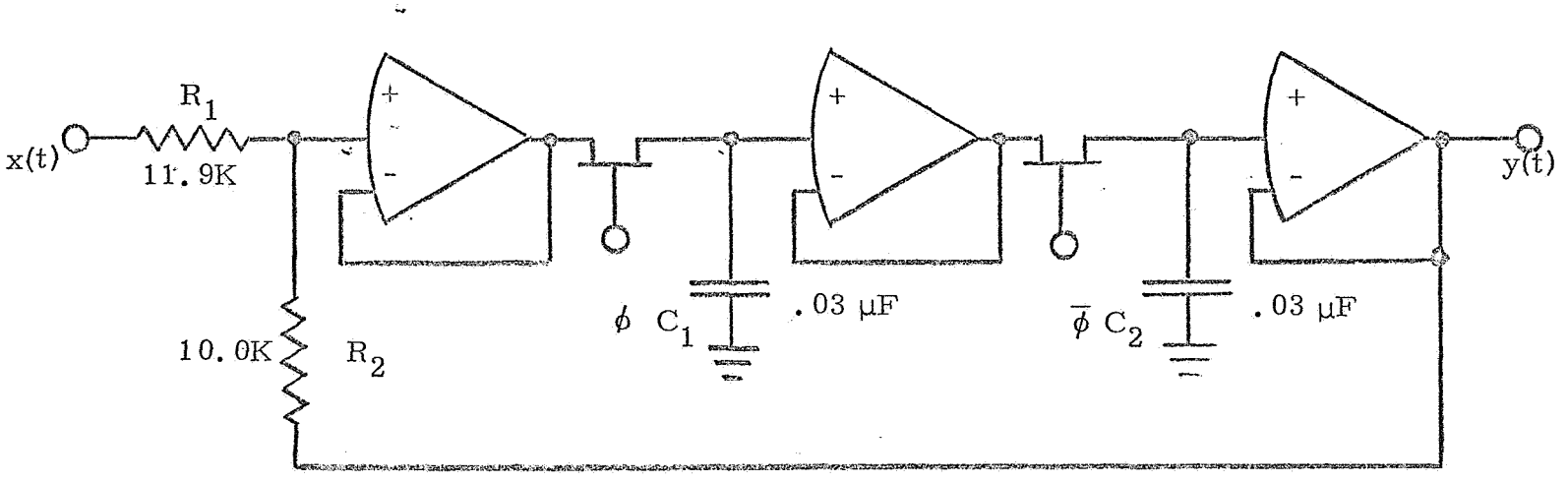

Figure 7c. First Degree Digital Filter

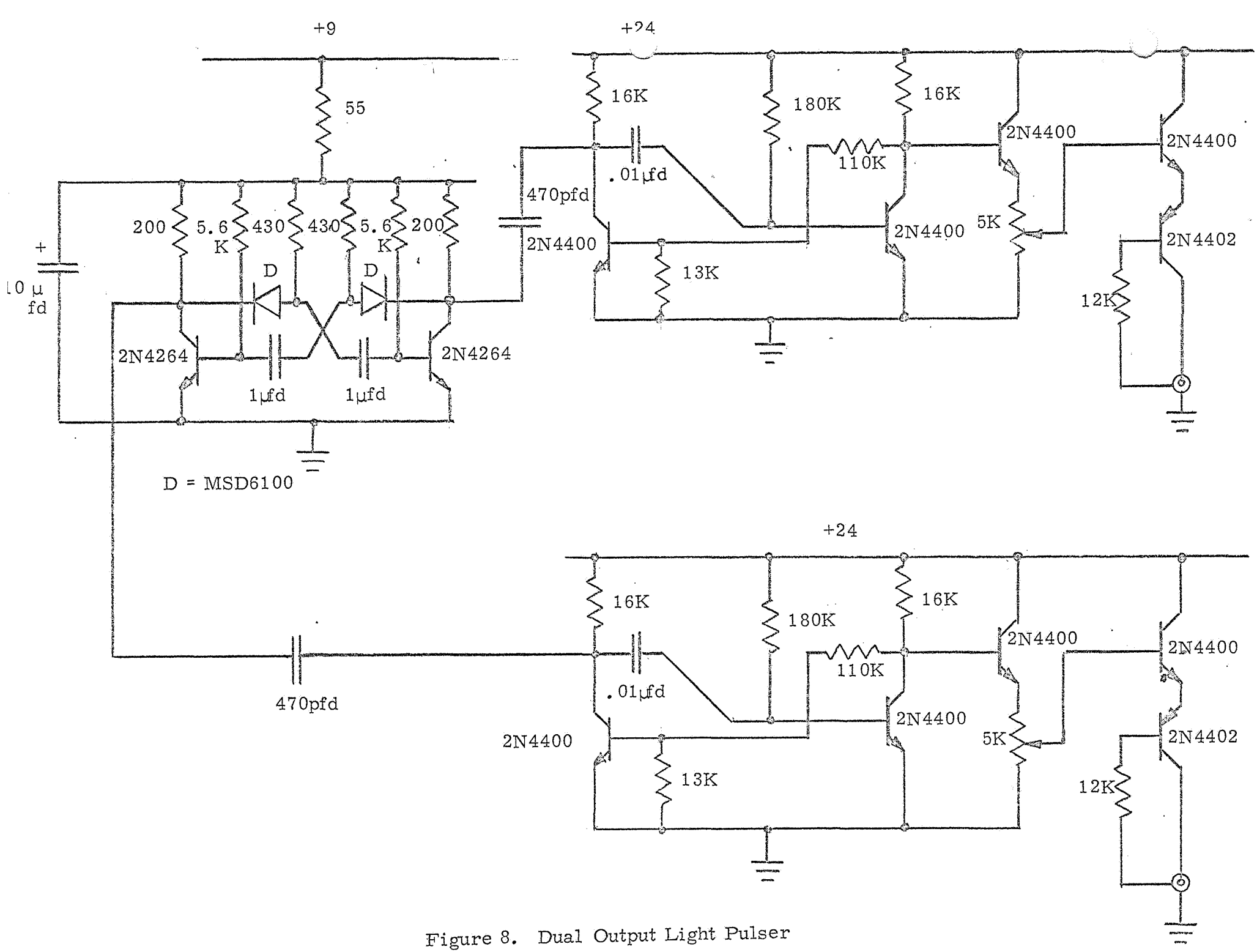

Figure 8. Dual Output Light Pulser